Organic & Biomolecular Chemistry

Accepted Manuscript

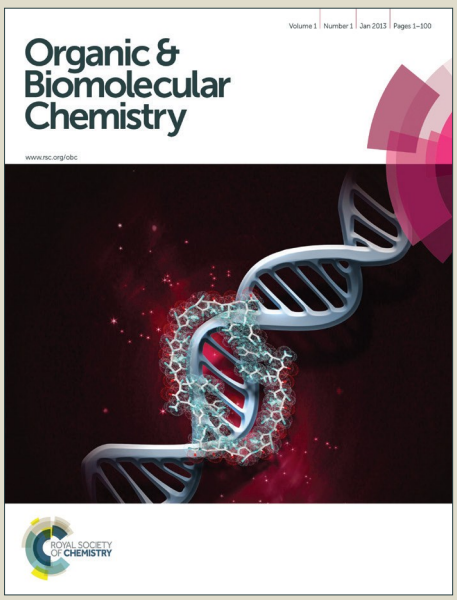

ROYAL SOCIETY OF CHEMISTRY

www.rsc.org/obc

Journal Name

ARTICLE

Chiral, triformylphenol-derived salen-type [4 + 6] organic cages†

M. Petryk,[a,b] J. Szymkowiak,[a,b] B. Gierczyk,[a] G. Spólnik,[c] Ł. Popenda[d], A. Janiak[a]* and M. Kwit[a,b]*

Received 00th January 20xx,
Accepted 00th January 20xx

DOI: 10.1039/x0xx00000x

www.rsc.org/

A one-pot synthesis of chiral [4 + 6] tetrahedral cage compounds containing a salen fragment on each face is presented. The formation of the [4 + 6] products remains in contrast to reaction of 1,3,5-triformylphloroglucinol with chiral diamines where [2 + 3] keto-enamine pseudocyclophanes are formed exclusively. The presence of OH groups determine the structural and spectroscopic properties of these cage compounds while a change in the reaction conditions facilitates the isolation of the microcrystalline products of specific surface area varying from 5 to 578 $m^2 g^{-1}$.

Introduction

The self-assembly of small, structurally predisposed substrates into larger 3D supramolecular cage-like products, resembling Platonic or Archimedian solids has attracted unprecedented attention during the last decade.[1] In contrast to the irreversible C-C bond formation, the reversible imination is an attractive alternative synthetic way for obtaining large symmetric macrocycles and organic molecular cages (OMCs), using relatively simple building blocks.[2,3] The choice of suitable building blocks is crucial for the rational planning of the synthesis and for modeling specific properties of the OMCs. For instance, the use of a tripodal aldehyde – 1,3,5-triformylbenzene and optically pure vicinal diamines provides a class of chiral molecular [4 + 6] cages characterized by unusual (for pure organic compounds) *T* symmetry.[4] Extension of the aldehyde structure leads to cages that differ in amine-aldehyde stoichiometry and have substantially larger molecular volumes.[5] This however, is at the expense of their stability.[6] The presence of OH group in the aldehyde skeleton has a profound effect on the structure and properties of the synthesized OMCs. Recently, Lisowski reported the synthesis of [2 + 3] condensation products in the reaction of 1,3,5-triformylphloroglucinol with vicinal diamines.[7] The observed [2 + 3] over the expected [4 + 6] selectivity remains opposed to the previously postulated "odd-even" rule[8] and is attributed to the presence of three OH groups in each aromatic ring.

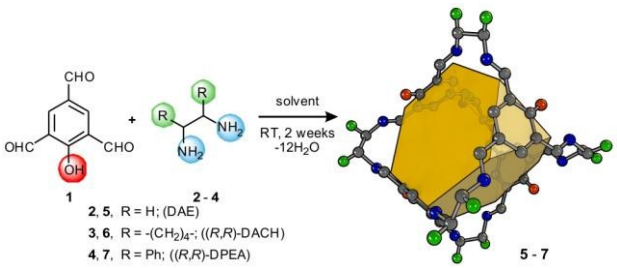

Scheme 1 Synthesis of organic molecular cages **5**-**7**.

Results and Discussion

Continuing on in our interest in chiral, functionalized macrocyclic compounds[9] we decided to extend our investigation into 3-dimensions, and to synthesize OMC's containing one salen unit at each face of the cage. We chose 2-hydroxy-1,3,5-triformylbenzene (**1**)[10] and 1,2-diaminoethane (DAE, **2**), *trans*-(1*R*,2*R*)-1,2-diaminocyclohexane (DACH, **3**) and (1*R*,2*R*)-diphenylethylenediamine (DPEA, **4**) as donors for synthesis of compounds **5**-**7** (Scheme 1).

The most convenient method of synthesis relies on the slow addition of finely pulverized **1** (2 *eq*) to a 0.014M solution of the amine (3 *eq*) in DMSO or chloroform-DMSO mixture and leaving the solution to stir at room temperature under an inert atmosphere. The optimal reaction time was estimated to be approximately two weeks based on ^{1}H NMR spectra measured at regular time intervals. Products **5** and **6** were isolated quantitatively by evaporation of the solvent. A further purification of **5** was carried out using solid-liquid extraction (over a two-week period) with the aid of a Soxhlet apparatus and large quantities of chloroform. An analytically pure sample of **6** was obtained by slow diffusion of diethyl ether vapors into a saturated chloroform solution of **6**. The cage **7**, precipitated as an orange microcrystalline powder with 35% yield. Evaporation of the filtrate provided the remaining portion of the product. Dried under high vacuum and in elevated

[a] *Department of Chemistry, Adam Mickiewicz University, Umultowska 89B, 61 614 Poznań, Poland, e-mail: agnieszk@amu.edu.pl or marcin.kwit@amu.edu.pl.*
[b] *Wielkopolska Center for Advanced Technologies (WCAT), Umultowska 89C, 61 614 Poznań, Poland.*
[c] *Institute of Organic Chemistry Polish Academy of Sciences, Kasprzaka 44/52, 01 224, Warszawa, Poland.*
[d] *NanoBioMedical Centre, Adam Mickiewicz University, Umultowska 85, 61 614 Poznań, Poland.*

† Dedicated to Prof. Bogdan Marciniec on the occasion of his 75 birthday.

Electronic Supplementary Information (ESI) available: experimental procedures, calculation details, copies of NMR, MS and IR spectra, Figures SI_1-SI_38, X-ray, PXRD and TGA data, full Gaussian citation, tabulated total and relative energies for calculated structures and Cartesian coordinates. CCDC 1477553. See DOI: 10.1039/x0xx00000x

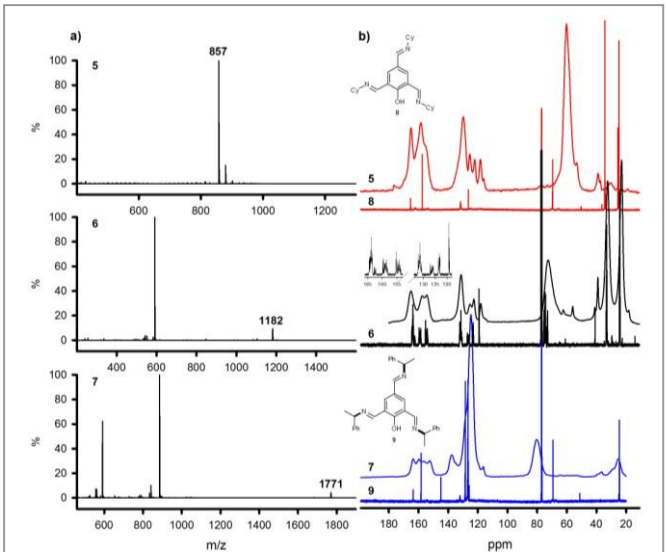

Figure 1 ESI-TOF mass spectra of cages **5**-**7** a) and the comparison of ^{13}C NMR spectra measured for solid **5** and solute of **8** (red lines), solid and dissolved **6** (black lines) and solid **7** and solute of **9** (blue lines) b). Insert shows the aromatic region of ^{13}C NMR spectrum of **6**.

temperature products **5** and **7** are virtually insoluble in common organic solvents and were characterized by (HR)MS, FT-IR, ^{13}C CPMAS NMR spectra. The FT-IR and ^{13}C CPMAS NMR spectra of **5**-**7** were compared with those measured for solutions of model compounds **8** and **9** (Figure 1).

The two C=O stretching bands observed at 1684 and 1661 cm^{-1} in FT-IR spectrum of the parent aldehyde **1** disappeared after imination. In the FT-IR spectra of **5**-**7** we did not observe any signals for neither the free amine nor the aldehyde. The characteristic imine stretching bands appeared at 1634 and 1601 cm^{-1}, in full consistency with the IR spectrum of the model imine **8** (Figures SI_1-SI_2, ESI).

ESI-TOF analyses showed $[M+H]^+$ molecular ions at m/z = 857, 1182 and 1771, respectively for **5**-**7**, corresponding to a 4 + 6 (12 imine bond formation) condensation stoichiometry (Figure 1a). Due to the presence of twelve nitrogen atoms, the cages **5**-**7** are able to over-protonate. The highest-intensity peaks in the MS spectra corresponded to $[M+2H]^{2+}$ molecular ions for cages **6** and **7**. It is noteworthy that the triply charged ion in the ESI-TOF spectrum of cage **7** was observed as well. For **5**, only a single charged ion was observed together with $[M+Na]^+$ sodiated ion (see Figures SI_3-SI_5, ESI). The elemental composition of each cage was confirmed by high-resolution mass spectra.

The ^{13}C CPMAS NMR spectra recorded for cages **5** and **7** were compared with ^{13}C NMR spectra measured in $CDCl_3$ for **8** and **9**. All characteristic signals for **5** and **7**, **8** and **9** appeared in the same spectral regions, regardless of the method of recording, thereby confirming the postulated structures of the cages (see ESI for details). Owing to the solubility in $CDCl_3$ we were able to directly compare the ^{13}C NMR spectra measured for solid and dissolved samples of **6**. Both spectra are in excellent agreement apart from the aromatic region of ^{13}C and ^{1}H NMR spectrum of **6**. More signals were observed than were expected for D_2 symmetry, the highest available for this particular OMC. Since the [4 + 6] stoichiometry is not in doubt,

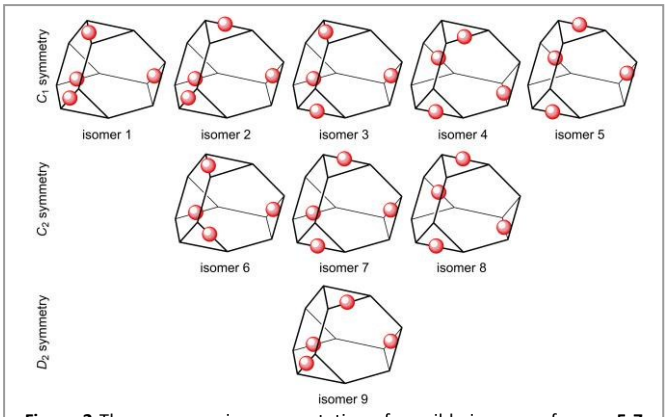

Figure 2 The macroscopic representation of possible isomers of cages **5**-**7** differing by position of hydroxyl groups represented here as red balls.

the possible reason for the signal multiplication is the presence of several structures of the same molecular formula that differ in symmetry. Taking the truncated tetrahedron as macroscopic representation of the molecular cages **5**-**7** and systematically decreasing its symmetry by adding the hydroxyl group (one for each triangular side) we obtained 4-combinations with the repetition of three elements corresponding to fifteen possible isomers that could be characterized either by trivial C_1 (isomers 1-5), C_2 (isomers 6-8) or D_2 (isomer 9, Figure 2) symmetries.

The presence of symmetry non-equivalent structures is clearly seen in the crystal structure of **6** (Figure 3). Cage **6** crystallizes in the cubic space group $F4_132$ with one-eighth of a molecule in the asymmetric unit. In the crystal, the molecule occupies 23 site symmetry position (Wyckoff notation 8a)[11] that is higher symmetry than is allowed and which consequently

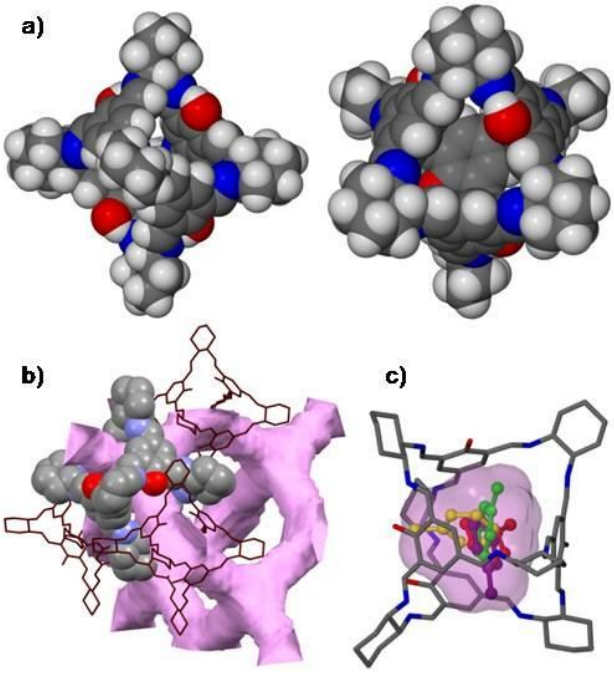

Figure 3 The molecular shape of cage **6** a). Only one position of the disordered hydroxyl group is shown; 3-D diamondoid channels drawn with a probe of 1.2 Å radius b); disordered solvent molecules entrapped in the cage cavity of 62.4 Å3 (r_{probe}=1.5 Å) c).[12] Due to the high disorder of the solvent molecules, their contributions were removed from the diffraction data using the Squeeze.[13]

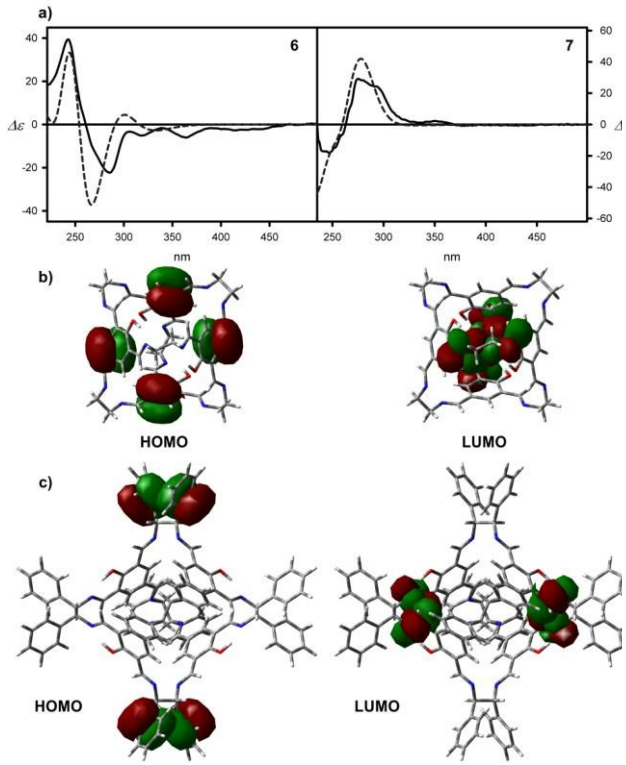

Figure 4 ECD spectra of cages **6** (left column) and **7** (right column) measured in chloroform solution (solid black lines) and calculated (dashed lines) at the IEFPCM/TD-CAM-B3LYP/6-311G(d,p) level a). Orbitals involved in electronic transitions responsible for negative Cotton effect observed at 270 nm in **6** b) and positive Cotton effect appeared at 270 nm in **7** c). The tetramethylene chains in **6** were replaced by hydrogen atoms.

leads to the appearance of disorder in certain parts of **6**. In particular, this is clearly evident in the site occupancy of the hydroxyl group that is split over three positions on the aromatic ring and in the large thermal ellipsoids of two carbon atoms in cyclohexane ring. Cage **6** has an outer diameter of 20.1 Å and an inner diameter of 8.3 Å. It contains four triangular windows each of approximately 5.8 Å. The size of the window is large enough to allow the entry of small and medium-sized solvent molecules into the interior of the cage with volume 62.4 Å^3.[12]

The presence of hydroxyl groups in the cage skeleton does not influence the self-assembly mode in the crystal. Similarly to the known cage **CC3-R**,[8] cage **6** packs in a window-to-window fashion giving rise to a 3-D diamondoid network of channels which are filled with the solvent molecules (Figure 3b and c). This corresponds to 14.1% (1.2 Å probe radius) of the unit cell volume that can be occupied by solvent molecules.[14]

Calculations at the IEFPCM/B3LYP/6-311G(d,p)[15] level of theory, suggests the appearance of each symmetry-different isomer in the reaction mixture, in accordance with the experimental data (see Table SI_3, ESI). In all of the cases studied here, the calculated lowest-energy structures are characterized by symmetries lower than D_2 (see Figures SI_24 and SI_25, ESI) and is either C_1 (**5**, isomer 3) or C_2 (cages **6** and **7**, isomer 6).

The optically active cages **6** and **7**, characterized by the same *R* absolute configuration at the stereogenic centers, show opposite (-/+ and +/-) sequences of the Cotton effects (CE's) in

Table 1 Measured for activated **7** Brunauer-Emmett-Teller surface areas (SA_{BET}) as a function of reaction conditions.[a]

	Solvent percentage content			SA_{BET} [m^2 g^{-1}]
Entry	DMSO	$CHCl_3$	H_2O	
1	100	0	0	12.5
2	75	25	0	6.3
3	50	50	0	5.3
4	25	75	0	6.6
5	97.5	0	2.5	254.1
6	95.0	0	5.0	354.4
7	92.5	0	7.5	368.2
8	90	0	10	577.8

[a]**1** - 2 mmol, **4** - 3 mmol, RT, inert atmosphere, RT, 2 weeks; the total solvent volume - 50 mL.

the region of strong electronic absorption (300-230 nm, see Figure 4a). In **6**, the CE's appear between 300 and 230 nm and originate solely from exciton interactions between aromatic units.[16] The π–π* electronic transition responsible for negative CE involves HOMO to HOMO-3 and LUMO+4 to LUMO+7 molecular orbitals, as revealed by DFT calculations.[15] Positive rotatory strength, generated by higher-energy electronic transitions, involved HOMO-3–HOMO-6 and LUMO–LUMO+3 orbitals (Figure 4 and ESI).

The ECD spectrum of **7** analyzed with the use of exciton chirality formalism led to conclusion that the interactions between aryloimine units are overwhelmed by exciton coupling between electric transitions dipole moments polarized along the long axis of phenyl located at vertices of the tetrahedron.

The sign of the long-wavelength exciton Cotton effect in **7** is in accordance with the positive helicity of C_{ar}-C*-C*-C_{ar} torsion angle. However, the π–π* electronic transitions responsible for the positive Cotton effect at 250 nm is of CT character and involved HOMO orbitals localized at phenyl substituents and LUMO's localized at aryloimine units as revealed by DFT calculations. Thus, the use of empirical exciton chirality rule, although gave the qualitatively correct answer, is not sufficient to explain the origin of observed phenomena.

The measured and calculated at the IEFPCM/TD-CAM-B3LYP/6-311G(d,p) level ECD spectra for **6** and **7** are in almost perfect agreement, additionally confirming the postulated molecular structures.

Although this report focuses mostly on the synthesis and structure of **5**-**7**, it is worth mentioning the macroscopic properties, namely the Brunauer-Emmett-Teller surface area (SA_{BET}), placing particular emphasis on cage **7**. Cage **7** precipitated from the reaction mixture, giving the "raw" product whose structure may be affected by the reaction conditions (solvent) but was not changed during further processing. In the first set, we started from absolute DMSO and gradually increased the proportion of chloroform in the reaction mixture from 0 to 100% (see Table 1, entries 1-4). In the second set, we again use the absolute DMSO and controlled the amount of water (Table 1, entries 5-8). The "raw" samples show a sharp step in the TGA curves upon

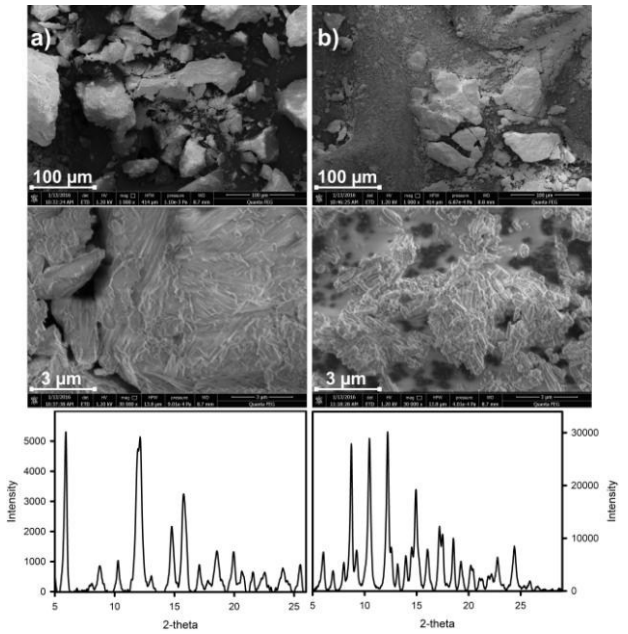

Figure 5 SEM images and PXRD data of material derived from **7**, characterizing by the lowest (a) and the highest (b) value of SA_{BET}.

heating to 100 °C, which corresponds to the removal of solvent molecules from the pores.

The initial attempts to obtain porous material with the use of a DMSO-chloroform mixture, as the reaction solvent, were unsuccessful. The estimated values of SA_{BET} were below 10 m^2 g^{-1} when the percentage content of chloroform ranged from 25 to 75%. Contrasting results were obtained for the second set. Even small amounts of water (2.5% v/v) significantly affected measured SA_{BET} values. The highest SA_{BET} value (578 m^2 g^{-1}) was obtained when the water content was up to 10% of the total solvent volume. This corresponds to more than 20% of the weight loss upon heating of the "raw" material.

Two extreme examples of the material obtained from **7** that are characterized by the lowest and the highest SA_{BET} values (entries 1 and 8, Table 1) were analyzed by scanning electron microscopy (SEM) (Figure 5). At low magnification, the bulk structure of both materials is similar. The SEM photographs exhibited the presence of irregular structures having lateral dimensions up to 100 microns. A more significant difference is visible at a higher magnification. While the material of low SA_{BET} value (Figure 5a) does not exhibit any defined structure, the SEM photograph of the material of high SA_{BET} value indicated microcrystalline character, confirmed by PXRD measurements. The average height of the microcrystals does not exceed 1 µm.

Conclusions

Herein we have shown an efficient synthetic route that provides a new class of chiral organic cage compounds, characterized by the ease of modeling the bulk properties. These cages are synthesized by two-week imination reactions between symmetric triformylphenol and vicinal diamines. Despite the reaction time, the products are obtained as approximately equimolar mixtures of isomers differing only in molecular symmetry. The extension of the reaction time up to three months did not affect the distribution of the respective symmetry-different products and does not provide the product of the highest symmetry. This remains contrary to the proposed dominant role of entropy in symmetry as the factor that controls the structure and distribution of products having the same bond formation enthalpies.[17,18]

The results reported here represent a positive signal for the subsequent application of the test compounds in the nearest future, especially for selective gas sorption or for isomers separation. These studies are currently under progress in our laboratory and the results will be reported in a due course.

Acknowledgements

This work was supported by research grant from National Science Center (NCN) Poland no UMO-2012/06/A/ST5/00230. All calculations were performed in Poznan Supercomputing and Networking Centre (grant no 217).

Notes and references

1 selected reviews: (a) K. Kobayashi and M. Yamanaka, *Chem. Soc. Rev*., 2015, **44**, 449; (b) S. Zarra, D. M. Wood, D. A. Roberts and J. R. Nitschke, *Chem. Soc. Rev*., 2015, **44**, 419; (c) S. H. A. M. Leenders, R. Gramage-Doria, B. de Bruin and J. N. H. Reek, *Chem. Soc. Rev*., 2015, **44**, 433; (d) N. Ahmad, H. A. Younus, A. H. Chughtai and F. Verpoort, *Chem. Soc. Rev*., 2015, **44**, 9; (e) G. Zhang and M. Mastalerz, *Chem. Soc. Rev*., 2014, **43**, 1934; (f) N. M. Rue, J. Sun and R. Warmuth, *Isr. J. Chem*., 2011, **51**, 743.

2 S. J. Rowan, S. J. Cantrill, G. R. L. Cousins, J. K. M. Sanders and J. F. Stoddart, *Angew. Chem. Int. Ed*. 2002, **41**, 898.

3 (a) N. E. Borisowa, M. D. Reshetkova and Y. A. Ustynyuk, *Chem. Rev*., 2007, **107**, 46; (b) C. D. Meyer, C. S. Joiner and J. F. Stoddart, *Chem. Soc. Rev*., 2007, **36**, 1705; (c) M. E. Belowich and J. F. Stoddart, *Chem. Soc. Rev*., 2012, **41**, 2003; (d) Y. Jin, Q. Wang, P. Taynton and W. Zhang, *Acc. Chem. Res*. 2014, **47**, 1575; (e) S.-L. Huang, G.-X. Jin, H.-K. Luo and T. S. A. Hor, *Chem. Asian. J*., 2015, **10**, 24; f) L. J. Barbour, *Nature Chem.*, 2015, **7**, 97.

4 (a) P. Skowronek and J. Gawroński, *Org. Lett*., 2008, **10**, 4755; (b) T. Tozawa, J. T. A. Jones, S. I. Swamy, S. Jiang, D. J. Adams, S. Shakespeare, R. Clowes, D. Bradshaw, T. Hasell, S. Y. Chong, C. Tang, S. Thompson, J. Parker, A. Trewin, J. Bacsa, A. M. Z. Slawin, A. Steiner and A. I. Cooper, *Nat. Mater*. 2009, **8**, 973; (c) D. Holden, K. E. Jelfs, A. I. Cooper, A. Trewin and D. J. Willock, *J. Phys. Chem. C* 2012, **116**, 16639; (c) M. J. Bojdys, M. E. Briggs, J. T. A. Jones, D. J. Adams, S. Y. Chong, M. Schmidtmann and A. I. Cooper, *J. Am. Chem. Soc.* 2011, **133**, 16566.

5 H. Ding, Y. Yang, B. Li, F. Pan, G. Zhu, M. Zeller, D. Yuan and C. Wang, *Chem. Commun*. 2015, **51**, 1976.

6 K. E. Jelfs, X. Wu, M. Schmidtmann, J. T. A. Jones, J. E. Warren, D. J. Adams and A. I. Cooper, *Angew. Chem. Int. Ed*. 2011, **50**, 10653.

7 P. Kieryk, J. Janczak, J. Panek, M. Miklitz and J. Lisowski, *Org. Lett*. 2016, **18**, 12

8 (a) K. E. Jelfs, E. G. B. Eden, J. L. Culshaw, S. Shakespeare, E. O. Pyzer-Knapp, H. P. G. Thompson, J. Bacsa, G. M. Day, D. J. Adams and A. I. Cooper, *J. Am. Chem. Soc.* 2013, **135**, 9307; (b) T. Hasell, J.e A. Armstrong, K. E. Jelfs, F. H. Tay, K. M.

Thomas, S. G. Kazarian and A. I. Cooper, *Chem. Commun*., 2013, **49**, 9410.
9 (a) M. Kwit and J. Gawronski, *Tetrahedron: Asymmetry*, 2003, **14**, 1303; (b) M. Petryk, A. Troć, B. Gierczyk, W. Danikiewicz and M. Kwit, *Chem. Eur. J*., 2015, **21**, 10318; (c) A. Janiak, M. Petryk, L. J. Barbour and M. Kwit, *Org. Biomol. Chem*. 2016, **14**, 669.
10 A. A. Anderson, T. Goetzen, S. A. Shackelford and S. Tsank, *Synth. Commun*. 2000, **30**, 3227.
11 International Tables for Crystallography (Ed.: T. Hahn), Kluwer Academic publishers, Dordrecht, The Netherlands, 1996.
12 M. L. Connolly, *Science*, 1983, **221**, 701.
13 T. L. Spek, *ActaCrystallogr., Sect. A: Fundam. Crystallogr*., 1990, **46**, 194.
14 I. J. Bruno, J. C. Cole, P. R. Edgington, M. Kessler, C. F. Macrae, P. McCabe, J. Pearson, R. Taylor, *ActaCryst. B*, 2002, **58**, 389.
15 Gaussian 09, Revision D.01, Gaussian, Inc., Wallingford CT, 2009.
16 N. Harada, K. Nakanishi, Circularly Dichroic Spectroscopy – Exciton Coupling in Organic Stereochemistry, University Science Books, Mill Valley, 1983.
17 (a) S.-K. Lin, *J. Chem. Inf. Comput. Sci.,* 1996, **36**, 367; (b) J. Rosen, *Entropy*, 2005, **7**, 308; (c) S.-K. Lin, *Int. J. Mol. Sci*., 2001, 2, 10.
18 (a) P. Skowronek, B. Warżajtis, U. Rychlewska and J. Gawroński, *Chem. Commun*., 2013, **49**, 2524; (b) S. W. Sisco and J. S. Moore, *Chem. Sci*., 2014, **5**, 81.

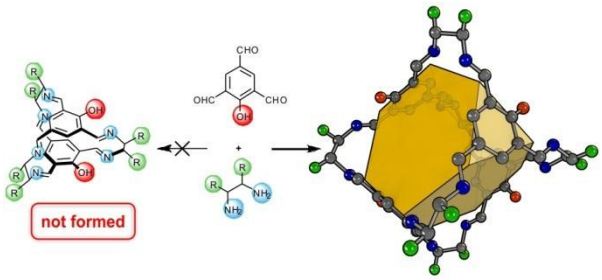

A new class of functionalized [4 + 6] tetrahedral imine cage compounds from triformylphenol and various vicinal diamines.